AIAA JOURNAL
Vol. 31, No. 4, April 1993

# Optimum Design of Forging Die Shapes Using Nonlinear Finite Element Analysis

C. S. Han,* R. V. Grandhi,† and R. Srinivasan‡
*Wright State University, Dayton, Ohio 45435*

**An optimization method is developed for the design of intermediate die shapes needed in the plane strain and axisymmetric forging operations. The approach is based on backward deformation simulation using nonlinear rigid viscoplastic finite element method and shape optimization techniques. The advantage of this optimization approach is that it has the ability to determine the intermediate die shapes from the final product shape by applying constraints on the plastic deformation of the material. This paper presents axisymmetric disk and plane strain case studies to demonstrate the new design procedures for minimizing variations in deformation rates during a multistage forging operation.**

## Nomenclature

$[B]$ = Shape function derivative matrix
$C_i$ = $B_{1i} + B_{2i} + B_{3i}$
$[D]$ = effective strain-rate coefficient matrix
$F_i$ = traction component
$\boldsymbol{F}$ = traction vector
$f_s$ = frictional stress
$[K]$ = stiffness matrix
$k$ = shear yield stress magnitude
$l$ = unit tangent vector
$m$ = friction factor
$P_{ij}$ = effective strain-rate tensor
$[P]$ = effective strain-rate matrix
$q_i$ = shape function
$Q$ = penalty constant
$S_c$ = tool-workpiece contact surface
$S_f$ = traction prescribed surface
$U_i$ = design variable
$u_i$ = velocity component
$u_o$ = velocity constant for numerical stability
$u_s$ = relative sliding velocity
$V$ = volume
$\boldsymbol{V}$ = preform nodal velocity vector
$v_i$ = nodal velocity component
$v_k$ = element nodal velocity vector
$x_i$ = component of cartesian coordinate
$\sigma_{ij}$ = Cartesian stress tensor
$\sigma'_{ij}$ = deviatoric stress tensor = $(\sigma_{ij} - \delta_{ij}(\sigma_{ii}/3)$
$\bar{\sigma}$ = effective flow stress magnitude = $\sqrt{3/2(\sigma'_{ij}\sigma'_{ij})}$
$\dot{\epsilon}_{ij}$ = strain rate tensor $= \frac{1}{2}\left(\frac{\partial u_i}{\partial x_j} + \frac{\partial u_j}{\partial x_i}\right)$
$\dot{\bar{\epsilon}}$ = effective strain-rate magnitude = $\sqrt{2/3(\dot{\epsilon}_{ij}\dot{\epsilon}_{ij})}$
$\dot{\epsilon}_v$ = volumetric strain-rate magnitude
$\dot{\epsilon}$ = strain-rate vector
$\delta$ = variational quantity
$\Pi$ = functional of power
$\Pi_p$ = penalty term in $\Pi$
$\Pi_D$ = deformation energy-rate term in $\Pi$
$\Pi_{Sc}$ = friction term in $\Pi$

Received Feb. 11, 1992; presented as Paper 92-2436 at the AIAA/ASME/ASCE/AHS/ASC 33rd Structures, Structural Dynamics, and Materials Conference, Dallas, TX, April 13-15, 1992; revision received July 20, 1992; accepted for publication July 30, 1992. 

*Research Associate, Department of Mechanical and Materials Engineering.
†Associate Professor, Department of Mechanical and Materials Engineering.
‡Assistant Professor, Department of Mechanical and Materials Engineering.

## Introduction

FORGING is a metal-forming process which causes change in the shape of the workpiece through the application of compressive forces. During closed die forging, the workpiece is deformed to fill die cavity representing the final component shape. Frequently in the design of a forging process, the only factors that are known are the final component shape, and the material with which it is to be made. These decisions are generally made without consultation with the die designer and are unalterable. The engineer has to then design a process which makes the desired part subject to limitations of shape, properties, cost, time, etc.

The starting billet shape for most forging operations is fairly simple: a bar with a round, a square, or a rectangular cross section. If the final component shape is complex, the billet cannot be deformed to the final shape in a single operation. To avoid various problems, such as incorrect material flow and fold over, excessive die forces, localized deformation, and improper die fill, the workpiece is deformed through several intermediate die shapes before the final product shaped die is used (Fig. 1). These intermediate shapes, variously referred to as the "buster," "blocker," or "finisher" shapes, are generally determined through extensive "trial-and-error." The intermediate die shapes obtained through the physical build-and-test approach are adequate for delivering the final part, but may not be the optimal shapes. The objective of this work is to find optimal intermediate die shapes based on constraints imposed on the variation of strain rates within the deforming object.

Among the methods available for the analysis of the metal-forming process, the finite element method (FEM) has the capability of producing detailed deformation information under combined mechanical and thermal loading, and solves a large variety of problems by changing the model and process parameters. The ability to quantitatively predict metal flow during large plastic deformation through finite element analysis has been available since the early 1980s, but these predictive capabilities have not been successfully used in the intelligent design of forging dies.

There have been many approaches to die design. The generally accepted empirical guidelines for the die design are published in handbooks,[1-3] where forgings and their preform shapes are classified according to their dimensional complex-

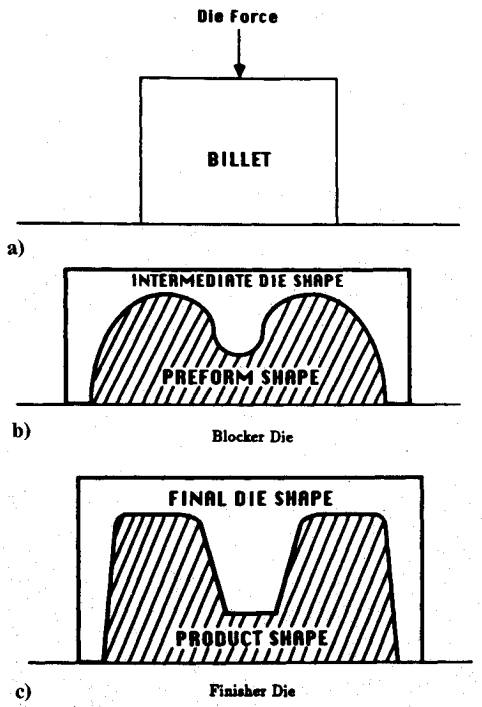


**Fig. 1 Billet, preform, and final product shapes.**

ities. These methods still require build and test procedures even for the known shapes but have limitations in giving guidelines for new materials and new product shapes.

Duggirala and Badawy,[4] and Duggirala[5,6] developed design procedures with the aid of a FEM simulation of the metal forming process using the program ALPID (analysis of large plastic incremental deformation). In this approach, the die shapes were initially designed by using empirical guidelines, then corrections are made based on the computer simulation result. This procedure was repeated until the desired properties were achieved in the formed shape. Since the finite element computer simulation eliminates build-and-test procedures, the cost and time in designing the intermediate die shapes were reduced considerably.

Hwang and Kobayashi[7-9] developed the backward tracing method for preform design. This method starts from the final product shape where the die is completely filled. The die is moved in reverse direction in an attempt to reverse the plastic deformation. During the actual forming simulation, a change in the boundary conditions occurs naturally when the nodal points on the workpiece come into contact with or leave the die. In backward tracing, workpiece boundary nodal points are initially attached to the die but need to be gradually detached. All of the workpiece surface nodes would become detached at the completion of the backward tracing process. This method was demonstrated for the case of a shell nosing operation, where the die shape is fairly simple. The method is not capable of handling more general die shapes. Since plastic deformation is an irreversible process, no natural path exists from the final workpiece shape to the starting billet. Specific paths may be selected by imposing constraints on the reverse deformation of the material. Improved design procedures based on the backward tracing method should include proper criteria for controlling the workpiece deformation. In this paper, a new approach called the backward deformation optimization method (BDOM) is developed by including design optimization strategies in the backward tracing method in releasing the nodes while satisfying the design constraints.

The present research focuses on the deformation control of the workpiece while reversing the deformation process from the final product shape. At every backward deformation step in the finite element simulation, the velocity profile of the die-contacting workpiece nodal points is determined by minimizing the maximum difference between the effective strain rate and the average effective strain rate. This process gives the information required to judge which workpiece node should be detached from the die to cause the optimum reverse path in forging. After successfully detaching workpiece nodes from the die, the backward tracing method is used to determine the workpiece geometry at the previous step. The iteration scheme is continued until most of the die-contacting nodes become free. The workpiece shape at that time is used as an intermediate die or preform shape. Depending on the complexity of the final product shape, several simulations may be required to determine several intermediate die or preform shapes. The resulting intermediate die shapes can provide smooth and complete die fill.

This paper describes the optimization problem formulation, design sensitivity analysis, and design variables. The design algorithm is implemented around the existing rigid viscoplastic finite element program ALPID. The predictions of the ALPID program have been experimentally verified for plane strain forging,[10] and the program has been successfully used for forging die design.[4-6] The theoretical background of the program is discussed briefly in the following section. Test problems are used to demonstrate the effectiveness of the intermediate die design procedures. Examples include an axisymmetric H-section forging and a plane strain U-section forging.

## Rigid Viscoplastic Finite Element Method

The present analysis is based on the rigid viscoplastic finite element method developed by Lee and Kobayashi[11] and extensions made for arbitrarily shaped dies by Oh.[12] The method has been successfully used in a variety of metal forming processes like forging and extrusion.[13] The formulation used in this method is briefly described below.

The constitutive law for viscoplastic materials relates the strain rate and deviatoric stress:

$$\dot{\epsilon}_{ij} = 3/2(\dot{\bar{\epsilon}}/\bar{\sigma})\sigma'_{ij} \tag{1}$$

The deformation energy due to rigid-plastic material behavior can be written as

$$\Pi = \int_V \bar{\sigma}\dot{\bar{\epsilon}}\, dV - \int_{S_f} F_i u_i\, dS \tag{2}$$

By taking the first-order variation of the functional,[14] the integral form of equilibrium equation is written as

$$\delta\Pi = \int_V \bar{\sigma}\delta\dot{\bar{\epsilon}}\, dV - \int_{S_f} F_i \delta u_i\, dS = 0 \tag{3}$$

Metal deformation occurs at a constant volume. Therefore, the admissible velocity $u_i$ needs to satisfy the incompressibility constraint. The constraints are imbedded in the variational form by introducing $Q$, a penalty constant. The modified first-order variation of the functional is given as

$$\delta\Pi = \int_V \bar{\sigma}\delta\dot{\bar{\epsilon}}\, dV + Q\int_V \dot{\epsilon}_v \delta\dot{\epsilon}_v\, dV - \int_{S_f} F_i \delta u_i\, dS = 0 \tag{4}$$

At the interface of the die and preform, the velocity boundary condition is given in the direction normal to the interface by the die velocity. Frictional forces at the interface between the workpiece and the dies represent the traction boundary condition. During metal forming, the frictional force at the interface cannot exceed the yield stress in shear of the workpiece material. Therefore, mathematically the frictional force is given by

$$f_s = mkl \cong mk\frac{2}{\pi}\tan^{-1}\left(\frac{|u_s|}{u_0}\right)l \tag{5}$$

where $m(0 \le m \le 1)$ is the friction factor.[13]

Finally, matrix representation of the governing equation for rigid viscoplasticity is

$$[K]V = F \tag{6}$$

where

$$[K] = \frac{\partial \Pi_D}{\partial v_i} + \frac{\partial \Pi_p}{\partial v_i} = \Sigma\left(\int_V \frac{\bar{\sigma}}{\dot{\bar{\epsilon}}} P_{ij}\, dV + \int_V QC_iC_j\, dV\right) \tag{7}$$

$$F = \frac{\partial \Pi_{S_F}}{\partial v_i} = \Sigma \int_{S_c} mk \frac{2}{\pi} q_j \tan^{-1}\left(\frac{q_j u_{sj}}{u_0}\right) dS \tag{8}$$

$[K]$ is the material and process-dependent nonlinear stiffness matrix. The solution to Eq. (6) is obtained iteratively.

## Backward Deformation Optimization Method

In the design of a forging process, the only information known beforehand is the final product shape and the material. The process engineer has to design the intermediate die shapes and the number of stages. Tracing from the final product shape to a simpler preform shape is one way of determining the intermediate die shapes.

The tracing of a workpiece shape from the final product shape is possible by reversing the die movement (Fig. 2). The velocity field is obtained by reversing the direction of nodal movement in forward simulation. The concept is shown in Fig. 3. The backward tracing method developed by Hwang and Kobayashi[7-9] iteratively checks whether the new workpiece geometry obtained by the backward simulation method would result in the starting shape upon repeating the forward simulation step. The procedure was repeated to trace back the initial shape. The algorithm was demonstrated for the shell nosing problem[9] where the die shape was fairly simple and the separation of nodes from the die in going from one step to the previous step was straightforward. But for a general complex die shape, a strategy is needed in releasing the nodes. This work develops a methodology called backward deformation optimization method (BDOM) for obtaining optimum intermediate die shapes. The backward tracing method was combined with numerical optimization techniques for releasing nodes and satisfying design constraints imposed on the deformation.

In the flow formulation of the metal forming, the state of deformation is fully described by the displacements, velocities, strains, and strain rates. Displacements depend on velocities and time increments, and strains are accumulated quantities based on strain rates and time increments. Strain rates are calculated using the strain rate-velocity equation of the continuous material in the velocity field. Therefore, the velocity of the workpiece nodal points and element strain rates are related by the strain rate-velocity equation. For this problem, the strain rate has been considered as the primary constraining function with the view to minimize the variation of strain rates within the workpiece during forging.

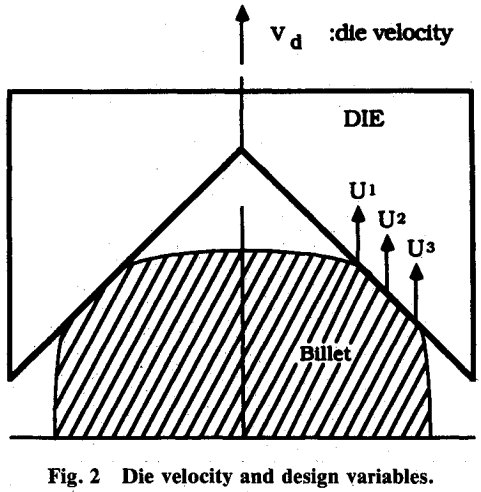


Fig. 2 Die velocity and design variables.

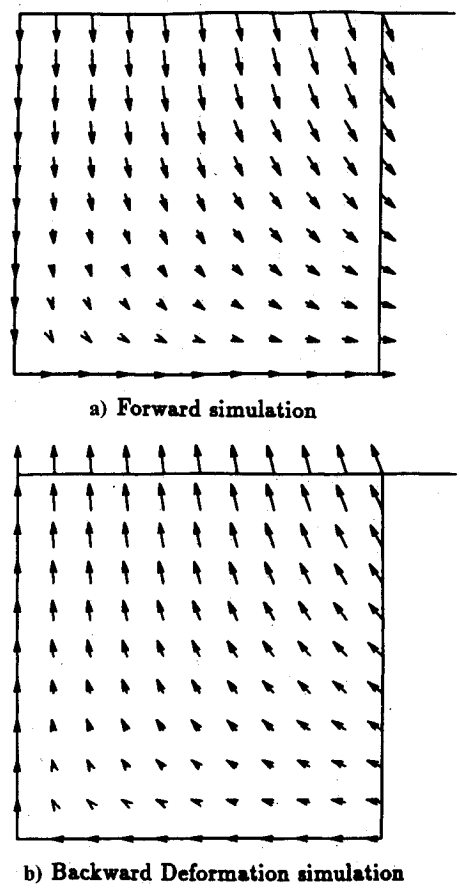

a) Forward simulation

b) Backward Deformation simulation

Fig. 3 Nodal velocity distributions.

To determine which node is to be detached from the die, the following technique, based on numerical optimization[15] is developed. During the backward deformation optimization process, die force or velocity is transmitted to the workpiece through the die contacting workpiece nodes. Although nodal velocities $U_1$, $U_2$, $U_3$, etc. shown in Fig. 2 are the same as the die velocity, their influence on the workpiece nodal velocities are quite different. Each die-contacting node is considered individually to calculate the influence of the die velocity on all of the workpiece nodal velocities using the analytical design sensitivity calculation method, and the detailed procedures are shown in the subsection on sensitivity analysis. The design variables in this problem are $U_i$, which are initially die velocities on the die-contacting workpiece nodes. Effective strain rates of each element are used as the design constraints.

### Optimization Problem

The design variables $U_i$ that minimize the maximum deviation of the effective strain rates from the average strain rates are determined. Mathematically, this mini-max problem[15] can be converted into the following minimization problem.

Find $U_i$ to minimize $H$ subject to the following inequality constraints:

$$|\dot{\bar{\epsilon}}_k - \dot{\bar{\epsilon}}_{\text{avg}}| \le H, \qquad k = 1, \ldots, n \tag{9}$$

where $\dot{\bar{\epsilon}}_k$ = $k$th element strain rate, $\dot{\bar{\epsilon}}_{\text{avg}}$ = average strain rate, $H$ = maximum difference in strain rates, and $n$ = number of elements, and side constraints on the design variables as:

$$0 \le U_i \le U_d, \qquad i = 1, \ldots, p \tag{10}$$

where $p$ is the number of boundary nodes and $U_d$ is the die velocity. This problem has $n$ design constraints and $p$ design variables.

The problem can be formulated as a linear programming problem by using the following linearization for the effective strain rates:

$$\dot{\bar{\epsilon}}_k = \dot{\bar{\epsilon}}_{k0} + \sum_{i=1}^{p} \frac{\partial \dot{\bar{\epsilon}}_k}{\partial U_i}(u_i - u_{i0}) \tag{11}$$

The $\dot{\bar{\epsilon}}_{k0}$ is the effective strain rate in $k$th element during the backward deformation optimization process, and $U_{i0}$ is the $i$th die-contacting nodal point velocity at the reference design. The initial design variables $U_{i0}$ are the same because they are the velocity of the die in the backward deformation optimization process. The above linear programming problem is solved by using the simplex method based routine DDPLS in IMSL library.

After solving the optimization problem, the node which shows the minimum velocity is detached from the die, because its contribution is the lowest in deforming the billet. The previous step workpiece geometry is determined by using the backward tracing method simulation after detaching the node. To maintain the solution not far from the linear solution, the timestep value is determined such that the strain increment in any element is less than the predetermined maximum strain increment. The optimization process and backward tracing process are continued until all of the nodes are separated from the die. The flow-chart of the optimization algorithm is shown in Fig. 4.

#### Sensitivity Analysis

The design sensitivity analysis procedure calculates the gradient of a function with respect to design variables. The design variables and constraint functions are nodal velocities of the die-contacting points and effective strain rates, respectively.

From the governing equation in rigid viscoplasticity shown in Eq. (6), the velocity vector, the stiffness matrix, and the traction force vector are implicit functions of die velocity.

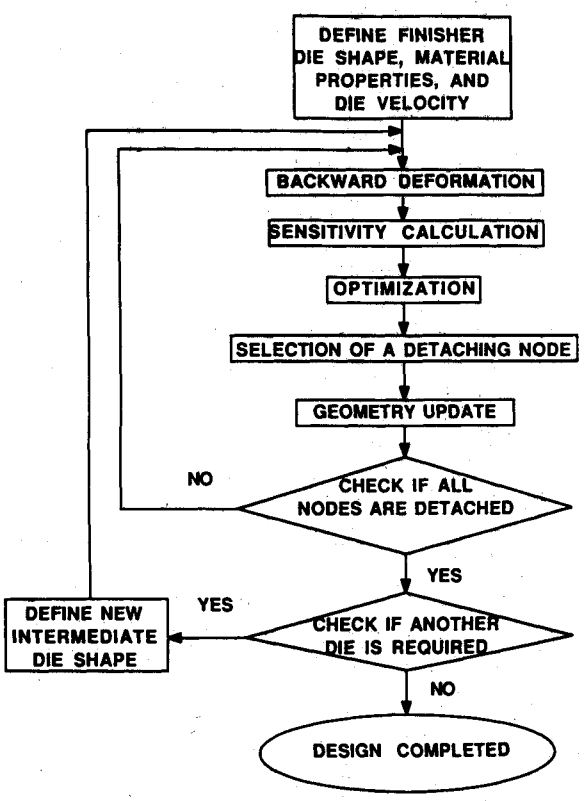


**Fig. 4 Intermediate die shape optimization flow chart.**

These quantities are differentiated with respect to workpiece die contacting nodal velocities. The resulting equation is

$$\frac{\partial V}{\partial U_i} = [K]^{-1}\left(\frac{\partial F}{\partial U_i} - \frac{\partial [K]}{\partial U_i} V\right) \tag{12}$$

Stiffness matrix and traction force vector derivatives are given as follows:

$$\frac{\partial [K]}{\partial U_i} V = \Sigma \int_V \left(\frac{1}{\dot{\bar{\epsilon}}} \frac{\partial \bar{\sigma}}{\partial \dot{\bar{\epsilon}}} - \frac{\bar{\sigma}}{\dot{\bar{\epsilon}}^2}\right) \frac{1}{\dot{\bar{\epsilon}}} P_{ik} V_k V_m P_{mj} \frac{\partial V_j}{\partial U_i} \, dV \tag{13}$$

$$\frac{\partial F}{\partial U_i} = \Sigma \int_S mk \frac{2}{\pi} q_i q_j \frac{u_0}{u_0^2 + (q_k u_{sk})^2} \frac{\partial}{\partial U_i}(V_j - U_j) \, dS \tag{14}$$

To relate the effective strain rates with the design variables, the effective strain rate is defined as follows using strain-rate components:

$$\dot{\bar{\epsilon}} = \sqrt{2/3}(\dot{\epsilon}_{ij}\dot{\epsilon}_{ij})^{1/2}$$

or alternatively in the matrix representation:

$$(\dot{\bar{\epsilon}})^2 = \dot{\epsilon}^T [D] \dot{\epsilon} \tag{15}$$

The diagonal matrix $[D]$ ) has $\frac{2}{3}$ and $\frac{1}{3}$ as its components, corresponding to normal strain rate and shear strain rate, respectively.

$$[D] = \begin{bmatrix} \frac{2}{3} & 0 & 0 & 0 \\ 0 & \frac{2}{3} & 0 & 0 \\ 0 & 0 & \frac{2}{3} & 0 \\ 0 & 0 & 0 & \frac{1}{3} \end{bmatrix}$$

The strain rate in each element can be derived using the strain-rate matrix $[B]$ and preform nodal velocity vector $v$:

$$\dot{\epsilon} = [B] v \tag{16}$$

Substituting Eq. (16) into Eq. (15) gives

$$(\dot{\bar{\epsilon}})^2 = v^T [B]^T [D][B] v = v^T [P] v \tag{17}$$

where $[P] = [B]^T [D][B]$.

Differentiation of Eq. (17) with respect to the design variable $U_i$ gives

$$\frac{\partial \dot{\bar{\epsilon}}_k}{\partial U_i} = \frac{1}{\dot{\bar{\epsilon}}_{k0}} v_k{}^T [P] \frac{\partial v_k}{\partial U_i} \tag{18}$$

In Eq. (18), $v_k$ is the nodal velocity vector for the $k$th element, and $\partial v_k / \partial U_i$, which is the nodal velocity sensitivity for the $k$th element, is obtained from Eq. (12). Equation (18) relates the change of constraint function to that of design variable.

## Numerical Results and Discussions

The shape optimization technique to determine the intermediate die shapes is demonstrated using two examples—an axisymmetric disk forging problem with a "H" cross-section and a plane strain channel forging problem with a "U" cross-section. A non-strain hardening material having the constitutive relation $\bar{\sigma} = 10\dot{\bar{\epsilon}}^{0.3}$ was used in this work. A constant shear force friction factor of 0.15 was assumed between the workpiece and the dies.

#### Example 1. Axisymmetric Forging Problem

The disk geometry shown in Fig. 5a has rotational symmetry about the centerline and is also mirror symmetric about the horizontal plane. The deformation of the upper part of Fig. 5b is representative of the entire disk forging problem. A cylindri-

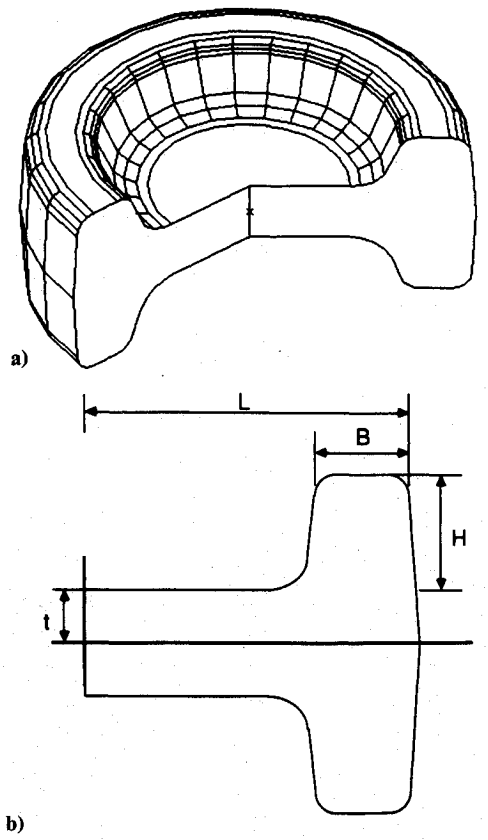


Fig. 5 Axisymmetric H-section.

cal billet of an equal volume is the starting shape for the problem, which has a radius of 4.71 in. and a height of 4.71 in. Also, the axisymmetric disk has a web thickness of 0.75 in., a rib height of 1.5 in., and a rib width of 1.5 in. The predicted workpiece shapes during forward simulation are shown in Fig. 6, by considering the final product shape as the die shape. The workpiece material separates from the die in the vicinity of the fillet (Fig. 6d). As a result of this, there is a possibility of a foldover towards the end of deformation (Fig. 6f). The forging of this part should, therefore, be conducted in two stages, i.e., the billet should first be deformed to an intermediate shape using a "blocker" die, and then to the final shape using the "finisher" die. The blocker die is designed using the shape optimization techniques developed in this work, as follows.

Figure 7a shows the workpiece completely filling the die. All surface nodes of the workpiece are in contact with the die. The surface nodes were grouped into three zones (marked as A, B, and C). Velocities of the end nodes of these lines are taken as the design variables.[16] The grouping of nodes results in smooth geometric shapes for the die by avoiding local kinks. At the beginning of the backward deformation step, the node on the symmetric plane (marked 1) is assumed to be separated from the die. The sensitivity of the effective strain rates of the workpiece elements is calculated with respect to the design variables. The linearized optimization problem is solved and the new nodal velocities are obtained. The design variable with the least velocity magnitude indicates that the corresponding node separates from the die contact in that timestep. Accordingly, that particular node is detached from the die.

Table 1 shows the effect of detaching a particular node on the strain-rate distribution in the workpiece. In the first step, the maximum strain rate decreased from 42.5/s to 17.8/s, the minimum strain rate decreased from 0.06/s to 0.03/s, and the average strain rate decreased from 1.58/s to 1.40/s. The range of strain rate distribution is decreased and a more uniform metal flow is realized. The geometry of the workpiece is updated then using the backward tracing method. In this procedure, as explained in the Introduction, the die is moved in the reverse direction. The equilibrium equations given in Eq. (6) are solved and modified workpiece nodal velocities are obtained. The workpiece geometry is updated using these velocities and timestep. It was found, for the particular problem considered in this example, that limit of maximum strain increment was reached before maximum allowable timestep. Table 1 presents results for four steps to demonstrate the optimization capability. In this problem, in fact, there were 30 timesteps before an intermediate die shape was determined.

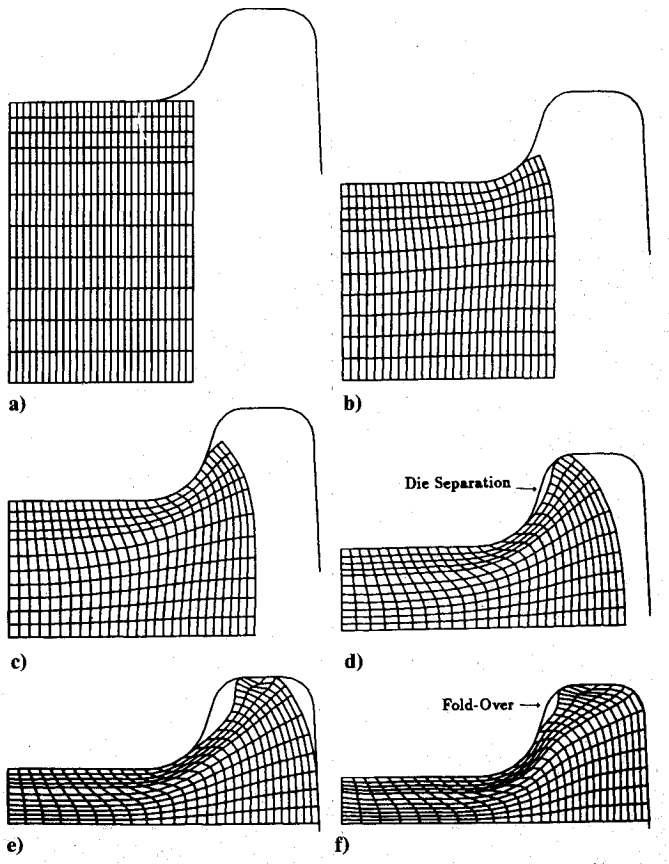


Fig. 6 Simulation of single-stage forging process in H-section.

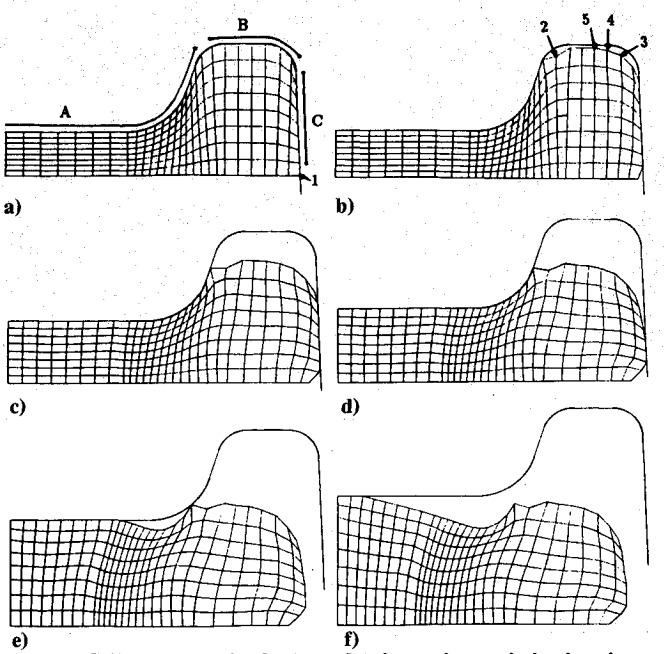


Fig. 7 Grid shapes during backward deformation optimization simulation in H-section.

The backward deformation optimization procedure indicates that the surface in contact with the top of the rib becomes free of the die, while the workpiece continues to slide along the vertical sides, as shown in Figs. 7c and 7d. Subsequently, the material on the outside edge separates from the die (Fig. 7e), and finally the web (horizontal) section separates from the die (Fig. 7f). The shape of the workpiece at this step is an intermediate shape from which the final shape can be forged with a minimum variation in effective strain rates.

To check the effectiveness of the Backward Deformation Optimization Method in designing intermediate die shapes, the two stage forging of this "H" cross section disk was simulated using ALPID. For the forward simulation, the intermediate shape determined by the optimization scheme was used as the die shape for the first stage of forging, and the resulting workpiece was then deformed to the final shape. The change in the workpiece geometry during the first stage of forging is shown in Figs. 8a–8c, and the forging of the intermediate shape to the final shape is shown in Figs. 8d–8f. It can be seen that in both stages, complete die fill is obtained. During the second stage forging, the top surface in the rib remains substantially horizontal, and the material slides up the vertical sides of the rib. Final die fill is obtained when the nodes on the top surface of the rib all touch the die, and the fold-over phenomenon is not observed.

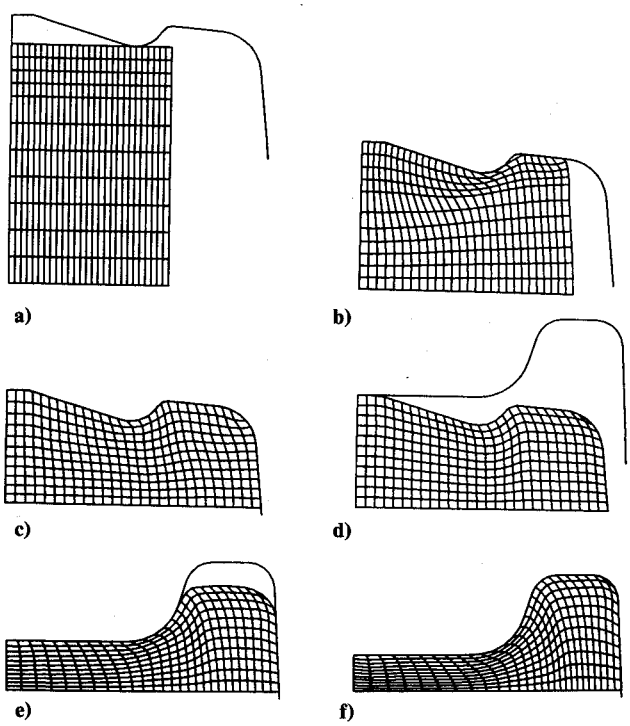


**Fig. 8 Simulation of optimized two-stage forging process in H-section.**

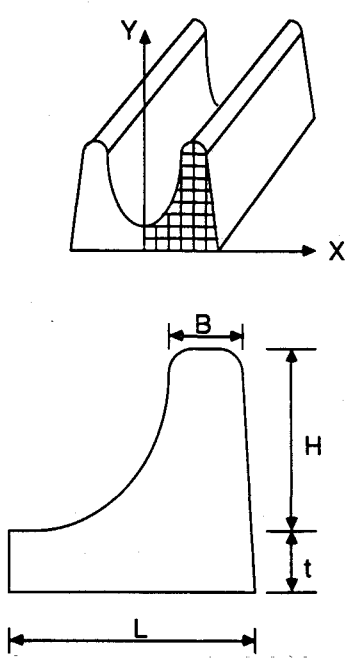


**Fig. 9 Plane strain U-section.**

**Table 1 Minimum, maximum, and average strain rates before and after optimization in H-section**

| Step no. | Max. $\dot{\bar{\epsilon}}_k$ | | Min. $\dot{\bar{\epsilon}}_k$ | | Avg. $\dot{\bar{\epsilon}}_k$ | |
|---|---|---|---|---|---|---|
| | Initial | Optimum | Initial | Optimum | Initial | Optimum |
| 1 | 42.5106 | 17.8744 | 0.0601 | 0.0343 | 1.5789 | 1.3979 |
| 2 | 17.1486 | 10.4878 | 0.0339 | 0.2652 | 1.3775 | 1.2520 |
| 3 | 10.3118 | 6.6620 | 0.2025 | 0.1223 | 1.2259 | 1.0748 |
| 4 | 6.5248 | 4.6047 | 0.1228 | 0.1749 | 1.0591 | 1.0023 |

**Table 2 Minimum, maximum, and average strain rates before and after optimization in U-section**

| Step no. | Max. $\dot{\bar{\epsilon}}_k$ | | Min. $\dot{\bar{\epsilon}}_k$ | | Avg. $\dot{\bar{\epsilon}}_k$ | |
|---|---|---|---|---|---|---|
| | Initial | Optimum | Initial | Optimum | Initial | Optimum |
| 1 | 46.3592 | 20.8354 | 0.0055 | 0.0110 | 1.0627 | 0.8168 |
| 2 | 19.9299 | 9.0361 | 0.0048 | 0.0052 | 0.7940 | 0.6818 |
| 3 | 8.7898 | 5.5988 | 0.0073 | 0.0062 | 0.6708 | 0.6172 |
| 4 | 5.7282 | 1.2261 | 0.0065 | 0.0076 | 0.6078 | 0.5003 |

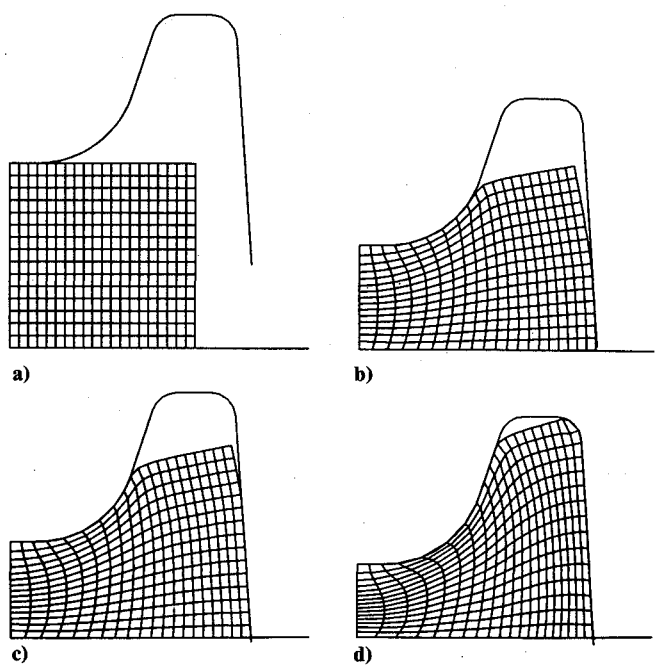


**Fig. 10 Simulation of single-stage forging process in U-section.**

The variance of total strain is reduced in the final product with the optimized two-stage forging compared to the single-stage forging from 0.1330037 to 0.075747, while average total strain is 1.22345 for single-stage forging and 1.44517 for two-stage forging, respectively.

**Example 2. Plane Strain Forging Problem**

The plane strain "U" cross-section is symmetric about the $Y$ axis (Fig. 9), and due to the symmetry, the deformation of the shaded area is used for the study of entire plane strain forging problem. The U-section has a web thickness of 1.5 in., a rib height of 4.5 in., and a rib width of 1.5 in. A rectangular

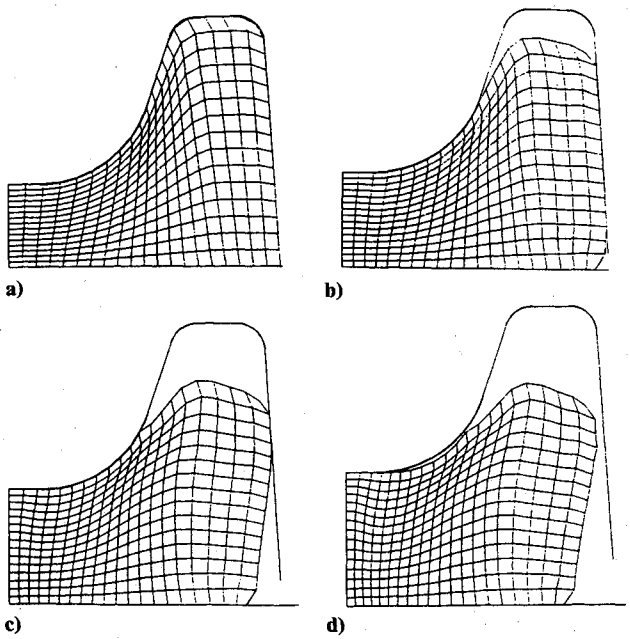


**Fig. 11 Grid shapes during backward deformation optimization simulation in U-section.**

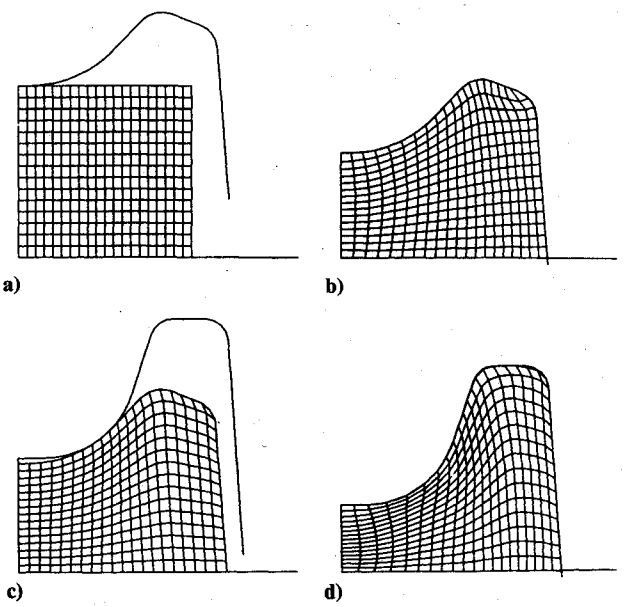


**Fig. 12 Simulation of optimized two-stage forging process in U-section.**

billet with an equal volume is used for the starting shape of the forging problem, and the billet has a width of 7.44 in. and a height of 3.72 in. The predicted workpiece configuration during forward simulation is shown in Fig. 10, and the die was not filled completely around inner part of rib due to flowing out of material before the closure of die. To fill die completely, the forging of this part should be done using an optimally designed intermediate die.

The blocker die is designed using the preform shape optimization technique developed in this work and the procedures are the same as given in the previous example. Die contacting workpiece nodes are gradually released as the backward deformation optimization simulation proceeds and the result is shown in Fig. 11. Table 2 shows the results for four steps to demonstrate the advantage of using optimization method in releasing nodes. For this problem, it took 26 timesteps before an intermediate die shape was determined.

To validate the effectiveness of optimally designed intermediate die, two-stage process simulations are conducted. The first-stage forging process using blocker die is shown in Figs. 12a and 12b, and the forging of the resulting preform to the final shape is shown in Figs. 12c and 12d. Relatively horizontal material movement was observed in the upper part of the rib during the second-stage forging operation, and the vertical part of the rib section remained on a straight line until it contacts with the finisher die. Die fill was observed in the two-stage forging operation, which was a serious problem in the one-stage forging operation.

## Summary

A technique for the design of intermediate forging die shapes using backward deformation simulation and design optimization was developed. The technique uses constraints imposed on the variation of effective strain rates in the workpiece to select a particular path for reversing the plastic deformation that occurs during forging.

As a first demonstration problem, the intermediate die designed for the forging of an axisymmetric disk was used to simulate the two-stage forging of the disk from a cylindrical billet. The results of this simulation with that of a single-stage forging showed that the optimized die avoided problems like foldover while reducing the variance of total strain in the final product. In the second demonstration problem, plane strain "U" section channel was used to show the advantage of using optimized two-stage forging. The result of optimized two-stage forging operation is compared with that of a single-stage forging operation. The comparison shows that complete die fill was obtained with optimized two-stage forging which was a problem with single-stage forging. Also, the variance of total strain distribution in the final product is reduced for the final product.

These examples illustrate that the backward deformation optimization method, using effective strain rate variation as the constraint, can be used to design intermediate die shapes in forging, while avoiding problems such as fold-over and incomplete die fill.

## Acknowledgments

This research work was done as part of CT-19 project "Design of Intermediate Shapes in Forging," sponsored by Edison Materials Technology Center (EMTEC). The authors acknowledge J. S. Gunasekera, Ohio University, Athens, Ohio; H. L. Gegel, S. M. Doraivelu, and A. Chaudhary of UES, Dayton, Ohio; and A. Shand, Harris Thomas Drop Forge Inc., Dayton, Ohio, for the technical comments provided during the course of this work.

## References

[1]Jones, R. C., "Drop Forging Die Design," The Association of Engineering and Shipbuilding Draftmen, Richmond, VA, 1965.

[2]Biswas, S. K., and Knight, W. A., "Towards an Integrated Design and Production System for Hot Forging Dies," *International Journal for Production Research,* Vol. 14, No. 1, 1979, pp. 23–49.

[3]Lange, K., *Closed Die Forging in Steel,* Springer-Verlag, Berlin, 1958.

[4]Duggirala, R., and Badaway, A., "Finite Element Method Approach to Forging Process Design," *Journal of Material Shaping Technology,* Vol. 6, No. 2, 1985, pp. 81–89.

[5]Duggirala, R., "Design of Forging Dies for Forming Flashless Ring Gear Blanks Using Finite Element Methods," *Journal of Material Shaping Technology,* Vol. 7, No. 1, 1990, pp. 33–47.

[6]Duggirala, R., "Using the Finite Element Method in Metal-Forming Processes," *Journal of Metals,* Vol. 42, No. 2, 1990, pp. 24–27.

[7]Hwang, S. M., and Kobayashi, S., "Preform Design in Plane-Strain Rolling by the Finite Element Method," *International Journal of Machine Tool Design Research,* Vol. 24, No. 4, 1984, pp. 253–266.

[8]Hwang, S. M., and Kobayashi, S., "Preform Design in Disk Forging," *International Journal of Machine Tool Design,* Vol. 26, No. 3, 1986, pp. 231–243.

[9]Hwang, S. M., and Kobayashi, S., "Preform Design in Shell Nosing at Elevated Temperatures," *International Journal of Machine Tool Manufacturing,* Vol. 27, No. 1, 1987, pp. 1–14.

[10]Jain, V. K., Matson, L. E., Gegel, H. L., and Srinivasan, R.,

"Physical Modeling of Metalworking Processes, Parts I and II," *Journal of Material Shaping Technology,* Vol. 5, No. 4, 1988, pp. 243–257.

[11]Lee, C. H., and Kobayashi, S., "New Solution to Rigid Plastic Deformation Problems Using a Matrix Method," *ASME Transactions, Journal of Engineering for Industry,* Vol. 95, Aug. 1973, pp. 865–873.

[12]Oh, S. I., "Finite Element Analysis of Metal Forming Processes With Arbitrarily Shaped Dies," *International Journal of Mechanical Science,* Vol. 24, No. 8, 1982, pp. 479–493.

[13]Kobayashi, S., Oh, S. I., and Altan, T., *Metal Forming and the Finite Element Method,* Oxford University Press, Oxford, England, UK, 1989.

[14]Reddy, J. N., *Energy and Variational Methods in Applied Mechanics,* Wiley, New York, 1984.

[15]Arora, J. S., *Introduction to Optimum Design,* McGraw-Hill, New York, 1989.

[16]Haftka, R. T., and Grandhi, R. V., "Structural Shape Optimization—A Survey," *Computer Methods in Applied Mechanics and Engineering,* Vol. 57, No. 1, 1986, pp. 91–106.